Title

Identifying reversible and irreversible magnetization changes in prototype patterned media using first- and second-order reversal curves

Journal

JOURNAL OF APPLIED PHYSICS, 103(7)

Authors

Winklhofer, Michael
Dumas, Randy K.
Liu, Kai

Publication Date

2008-03-11

DOI

10.1063/1.2837888

Peer reviewed

Identifying reversible and irreversible magnetization changes in prototype patterned media using first- and second-order reversal curves

Michael Winklhofer,[a] Randy K. Dumas, and Kai Liu
Physics Department, University of California, Davis, California 95616, USA

(Presented on 9 November 2007; received 12 September 2007; accepted 17 November 2007; published online 11 March 2008)

Arrays of nanomagnets have important potential applications as future generation ultrahigh-density patterned magnetic recording media, in which each nanomagnet constitutes a single bit. We introduce a powerful technique to identify and quantify reversible and irreversible magnetization changes, a key challenge in characterizing these systems. The experimental protocol consists of measuring a few families of second-order reversal curves along selected profiles in the first-order-reversal-curve diagram, which then can be decomposed into truly irreversible switching events and reversible magnetization changes. The viability of the method is demonstrated for arrays of sub-100-nm Fe nanomagnets, which exhibit complex magnetization reversal processes.
 [DOI: 10.1063/1.2837888]

Having the potential to reach unprecedented recording densities of 1 Tbit/in.[2] and beyond, patterned magnetic recording media have attracted a lot of interest in the last decade.[1,2] In future patterned media, the data are to be stored in arrays of nanomagnets such that, ideally, each nanomagnet holds 1 bit. With the lithographic techniques already available,[3] fundamental nonmagnetic parameters of the arrays such as grain size and nanomagnet spacing can be varied in a controlled fashion, which allows one to systematically study the effects of these parameters on the magnetic properties. Arrays of nanomagnets therefore also offer a unique opportunity to experimentally validate theoretical models of switching behavior, particle interactions, and thermal activation effects. To tackle these problems on a quantitative level, it is necessary to have a method that allows one to separate measured magnetization changes into contributions from irreversible and reversible processes.

We here propose an effective method for this task, which involves first-order and second-order reversal curves (FORCs and SORCs). A FORC (Refs. 4–8) is a magnetization curve $M(H_r,H)$, which originates at some reversal field H_r from the major loop $M(H)$, and SORCs (Ref. 4) are magnetization curves $M(H_r,H_q,H)$ branching off a given FORC at the second reversal field H_q. FORCs were originally introduced[9] to experimentally measure the Preisach distribution. Later, it was recognized that FORCs measured on magnetic systems consisting of curvilinear hysterons, such as the Stoner–Wohlfarth assemblage, cannot be fitted accurately by linear Preisach models. To overcome this limitation, Mayergoyz and Friedmann[4] suggested to measure also higher-order reversal curves in addition to FORCs, in particular, SORCs, and to fit a nonlinear, generalized Preisach model to both sets of curves.

Rather than fitting a model to measured sets of FORCs and SORCs, we here take a different approach and extract the amount of reversible and irreversible changes directly from the FORC and SORC data. For a given set of ascending FORC (increasing H, starting from H_r), the separation of reversible from irreversible magnetization changes can be performed only near the descending branch of the major loop, that is, for $H \to H_r$. Here, the irreversible change is the vertical difference between the major loop $M(H)$ and the FORC $M(H_r,H)$,

$$dM^{\mathrm{irr}}(H_r) = \lim_{H \to H_r} [M(H) - M(H_r,H)], \tag{1}$$

while the reversible change is

$$dM^{\mathrm{rev}}(H_r) = \lim_{H \to H_r} [M(H_r,H) - M(H_r)]. \tag{2}$$

The normalized difference $dM^{\mathrm{rev}}(H_r)/dH$, where $dH=H-H_r>0$, is also referred to as the reversible ridge.[10] To decompose the magnetization change along an ascending FORC at any $H>H_r$ into irreversible and reversible contributions, we suggest measuring a set of N descending magnetization curves $M[H_r,H_q(i),H]$, $i=1,\ldots,N$ branching off the particular FORC $M(H_r,H)$ after a second field reversal at $H_q(i)>H_r$. The amount of irreversible change in magnetization per field change $dH=H_q-H>0$ that occurred along the FORC near H_q is then the (vertical) difference between the SORC and the FORC

$$dM^{\mathrm{irr}}(H_r,H_q) = \lim_{H \to H_q} [M(H_r,H_q,H) - M(H_r,H)], \tag{3}$$

while the reversible change is obtained as

$$dM^{\mathrm{rev}}(H_r,H_q) = \lim_{H \to H_q} [M(H_r,H_q) - M(H_r,H_q,H)]. \tag{4}$$

To numerically determine the dM values from measured data sets, we fit a line to the initial segment of each reversal curve, that is, the first $(f+1)\times dH$ field steps from the reversal point onward, where f can be considered a smoothing

[a]Also at Department of Geosciences, University of Munich, D-80333 München, Germany. Electronic mail: michael@geophysik.uni-muenchen.de.

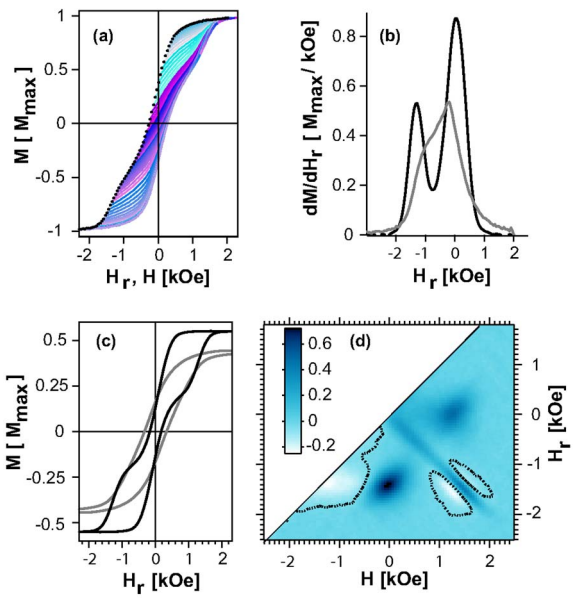

FIG. 1. (Color online) (a) A set of 125 ascending FORCs for the d_m =67 nm Fe nanodot sample, field spacing $dH_r=dH=50$ Oe. The origin $M(H_r,H=H_r)$ of each FORC is marked by a black dot. (b) Magnetization changes along descending-field branch of the major loop decomposed into reversible (gray) and irreversible (black) component using Eqs. (1) and (2). (c). Reconstructed reversible (gray) and irreversible (black) part of the major loop; ascending branch obtained by applying inversion operation to descending branch. (d) FORC function $\rho(H_r,H>H_r)$ in units of $M_{\max}/\mathrm{kOe}^2$, computed with a smoothing factor of 3. Regions where $\rho<0$ are enclosed by dotted contour lines.

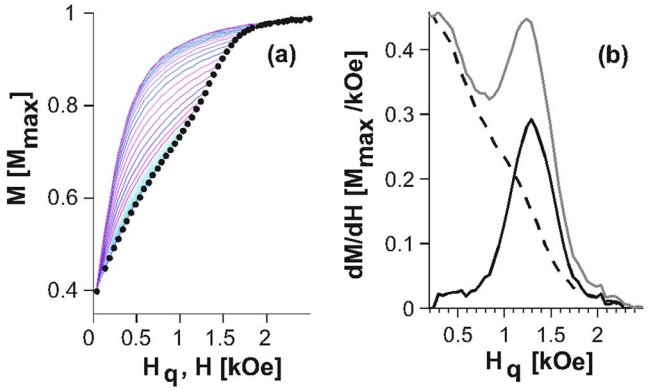

FIG. 2. (Color online) (a) A set of descending SORCs, $M(H_r,H_q,H)$, branching off an ascending FORC $M(H_r,H)$ with $H_r=40$ Oe. The origin of each SORC at $H=H_q$ is marked by a black dot, tracing out the FORC. (b) Irreversible (black solid) and reversible (black dashed) magnetization changes obtained by applying Eqs. (3) and (4) to the SORC data sets, in comparison with the total magnetization change $dM(H_r,H)/dH$ (gray line) along the corresponding FORC originating at $H_r=40$ Oe.

factor, as introduced by Pike *et al.*[5] to compute the FORC function from discrete FORC datasets.

We exemplify the method on arrays of sub-100-nm polycrystalline Fe nanodots, fabricated using a nanoporous alumina shadow-mask technique in conjunction with electron-beam evaporation.[11,12] By means of FORC diagrams, these arrays have already been characterized in detail[13,14] in terms of interactions, switching fields, and reversal mechanisms. The prevailing switching mechanism changes gradually from coherent rotation to vortex nucleation and annihilation as the mean dot size d_m increases from 52 to 67 nm.[13] The FORC diagrams also show that magnetostatic interactions in these arrays are practically negligible. The FORC diagram for the single-domain sample (d_m=52 nm) closely resembles that of a noninteracting Stoner–Wohlfarth assemblage.[7,15] Since Fe is a soft magnetic material and the easy axes of the dots are oriented at random in the plane, significant contributions to the magnetization from reversible processes can be expected. Therefore, the question arises as to what degree the features in the FORC diagrams reflect truly irreversible changes.

Figure 1 shows the FORC data set for the d_m=67 nm Fe nanodots (a). The outer boundary delineates the major hysteresis loop. Applying Eqs. (1) and (2) to the data sets, the slope along each FORC can be separated into reversible and irreversible components (b). The irreversible components, mostly along $H_r=0.1$ and -1.4 kOe, can be used to reconstruct the purely irreversible part of the major loop (c), which is even more constricted than the original one. The resulting FORC diagram (d) is reminiscent of the Preisach function predicted[16] and measured[9] for perminvar in that it has two large positive peaks offset from the $H=-H_r$ axis, about which they are symmetrically positioned. These two offset peaks—at $(H,H_r)=(1.3,0.1)$ and $(0.1,-1.4)$ kOe–result in a constricted major loop. The magnetization mechanisms underlying the two peaks are annihilation of a vortex from the same side as it was nucleated (upper peak) and nucleation of a vortex from negative saturation (lower peak).[13] The FORC diagram exhibits another interesting feature, a positive peak centered at $H=-H_r\sim 1.5$ kOe flanked by two smaller negative peaks. This negative-positive-negative trio of features can be explained statistically by a history-dependent distribution of annihilation fields,[17] or microscopically, by some shape anisotropy that leads to field polarity dependent annihilation fields.[13] Finally, there is a positive ridge centered at the $H=-H_r$ axis, extending from $H=0$ to $H=1$ kOe, which is related to coherent switching of single-domain particles in the sample. To clarify the nature of the prominent features in the FORC diagram in terms of reversible and irreversible processes, we measured sets of SORCs for several values of H_r and performed the decomposition into reversible and irreversible contributions according to Eqs. (3) and (4). An example is shown in Fig. 2 for $H_r=40$ Oe. It turns out that most of the magnetization changes for H near H_r, that is, $H_q<1$ kOe in Fig. 2(b), are due to reversible processes, manifested by the overlapping SORCs shown in Fig. 2(a). Irreversible processes (true switching events), on the other hand, are found to be associated with the upper of the two offset peaks in the FORC diagram, located at $(H,H_r)=(1.3,0.1)$ kOe, corresponding to the annihilation of vortices[13] that had nucleated at reversal field $H_r>40$ Oe.

In Fig. 3, the rate of irreversible (a) and reversible (b) changes is shown for four different sets of SORCs, attached to the FORCs originating at $H_r=+40$, -490, -940, and -1390 Oe, respectively. In (a), it can be clearly seen from the positive values that for those FORCs reversing at $H_r<0$, irreversible changes do occur during recoil to $H=0$, which means that the remanent magnetization $M(H_r,0)$ is not identical to the irreversible magnetization $M^{\mathrm{irr}}(H_r)$ for $H_r<0$. Moreover, the location of the left irreversible peak in each

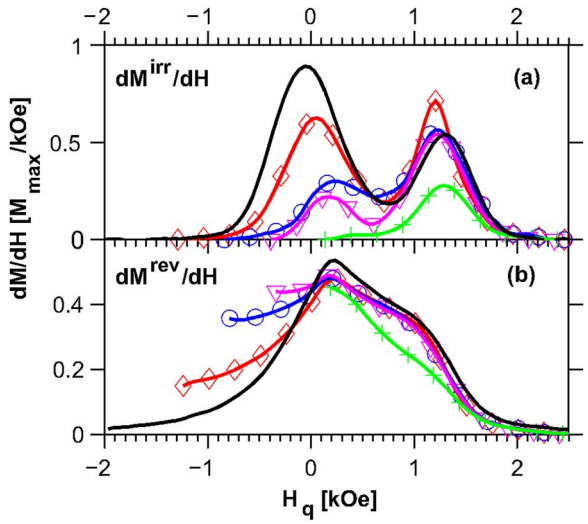

FIG. 3. (Color online) (a) Irreversible and (b) reversible magnetization changes along selected FORCs with H_r=40 Oe (+), −490 Oe (▽), −940 Oe (○), and −1390 Oe (◇), in function of the second reversal field H_q. Only every fifth data point is marked with a plot symbol. The slopes for the major loop from Fig. 1(b) (black line without plot symbols) are included in each figure for comparison.

curve is not stationary [Fig. 3(a)]. While the magnitude of the first peak (around 0 kOe) systematically increases as H_r becomes more negative, that for the second peak (around 1.4 kOe) shows much less appreciable variation with H_r and the peak location is almost stationary. Figure 3(b) reveals that the reversible slopes are not history independent, unlike often assumed. The only region where the reversible slope shows no apparent history dependence is the quadrant $Q_{+,-}$, defined by $H>0$, $H_r<0$, which implies that the mixed derivative $\partial^2 M^{\mathrm{rev}}/\partial H \partial H_r$ vanishes here. Therefore, the features in $Q_{+,-}$ of the FORC diagram [Fig. 1(d)] are due to irreversible changes. In particular, the negative-positive-negative trio of features in Fig. 1(d) has its origin mainly in irreversible processes as dM^{irr}/dH_q around H_q=1.5 kOe depends on H_r, while dM^{rev}/dH_q does not. This experimentally confirms the theoretical models.[13,17] To identify the characteristic of the positive and negative regions in the other quadrants of the FORC diagram, we again compare the H_r dependence of irreversible and reversible slopes from Fig. 3 and find that the negative and positive regions centered about $H \sim H_r \sim -1.4$ kOe and $\sim +60$ Oe, respectively, are due to reversible processes, while those lobes of the two peaks at $(H,H_r)=(1.3,0.1)$ and $(0.1,-1.4)$ kOe that are just outside $Q_{+,-}$ are due largely, but not solely, to irreversible processes (vortex nucleation and annihilation). These results demonstrate that the combination of FORC and SORC techniques can give very detailed information about the history-dependent irreversibility of magnetization changes.

We thank C. P. Li, I. V. Roshchin, and I. K. Schuller for the sample used in this study, and G. T. Zimanyi for useful discussions. This work was supported in part by BaCaTec, ACS (No. PRF-43637-AC10), and the Alfred P. Sloan Foundation.

[1] S. H. Sun, C. B. Murray, D. Weller, L. Folks, and A. Moser, Science **287**, 1989 (2000).
[2] C. A. Ross, Annu. Rev. Mater. Res. **31**, 203 (2001).
[3] J. I. Martin, J. Nogues, K. Liu, J. L. Vicent, and I. K. Schuller, J. Magn. Magn. Mater. **256**, 449 (2003).
[4] I. D. Mayergoyz and G. Friedmann, IEEE Trans. Magn. **24**, 212 (1988).
[5] C. R. Pike, A. P. Roberts, and K. L. Verosub, J. Appl. Phys. **85**, 6660 (1999).
[6] J. E. Davies, O. Hellwig, E. E. Fullerton, G. Denbeaux, J. B. Kortright, and K. Liu, Phys. Rev. B **70**, 224434 (2004).
[7] A. J. Newell, Geochem., Geophys., Geosyst. **6**, Q05010 (2005).
[8] M. Winklhofer and G. T. Zimanyi, J. Appl. Phys. **99**, 08E710 (2006).
[9] H. Wilde and H. Girke, Z. Angew. Phys. **11**, 339 (1959).
[10] C. R. Pike, Phys. Rev. B **68**, 104424 (2003).
[11] K. Liu, J. Nogues, C. Leighton, H. Masuda, K. Nishio, I. V. Roshchin, and I. K. Schuller, Appl. Phys. Lett. **81**, 4434 (2002).
[12] C.-P. Li, I. V. Roshchin, X. Batlle, M. Viret, F. Ott, and I. K. Schuller, J. Appl. Phys. **100**, 074318 (2006).
[13] R. K. Dumas, C.-P. Li, I. V. Roshchin, I. K. Schuller, and K. Liu, Phys. Rev. B **75**, 134405 (2007).
[14] R. K. Dumas, K. Liu, C.-P. Li, I. V. Roshchin, and I. K. Schuller, Appl. Phys. Lett. **91**, 202501 (2007).
[15] Y. X. Pan, N. Petersen, M. Winklhofer, A. F. Davila, Q. S. Liu, T. Frederichs, M. Hanzlik, and R. X. Zhu, Earth Planet. Sci. Lett. **237**, 311 (2005).
[16] R. Feldtkeller and H. Wilde, ETZ, Elektrotech. Z., Ausg. A **77**, 449 (1956).
[17] C. R. Pike and A. Fernandez, J. Appl. Phys. **85**, 6668 (1999).